

$\gamma^*N \rightarrow N(1710)$  transition at high momentum transfer

G. Ramalho and K. Tsushima

*International Institute of Physics, Federal University of Rio Grande do Norte, Avenida Odilon Gomes de Lima 1722, Capim Macio, Natal-RN 59078-400, Brazil*  
(Received 14 February 2014; published 18 April 2014)

In a relativistic quark model we study the structure of the  $N(1710)$  resonance, and the  $\gamma^*N \rightarrow N(1710)$  reaction focusing on the high momentum transfer region, where the valence quark degrees of freedom are expected to be dominant. The  $N(1710)$  resonance, a state with spin  $1/2$  and positive parity ( $J^P = \frac{1}{2}^+$ ), can possibly be interpreted as the second radial excitation of the nucleon, after the Roper,  $N(1440)$ . We calculate the  $\gamma^*N \rightarrow N(1710)$  helicity amplitudes, and predict that they are almost identical to those of the  $\gamma^*N \rightarrow N(1440)$  reaction in the high momentum transfer region. Thus, future measurement of the helicity amplitudes for the  $\gamma^*N \rightarrow N(1710)$  reaction can give a significant hint on the internal structure of the  $N(1710)$  state.

DOI: 10.1103/PhysRevD.89.073010

PACS numbers: 13.40.Gp, 12.39.Ki, 14.20.Gk

**I. INTRODUCTION**

The understanding of the electromagnetic structure of the hadrons, and its connection with the underlying degrees of freedom in quantum chromodynamics (QCD), are amongst two of the more interesting challenges in hadronic physics. Through the nucleon electroexcitation reactions,  $eN \rightarrow e'N^*$ , we can study the electromagnetic structure of the nucleon ( $N$ ) and the nucleon excitations ( $N^*$ ), including also the  $\Delta$  states. The excitation of nucleon resonances occurs through the intermediate processes  $\gamma^*N \rightarrow N^*$ , where  $\gamma^*$  is a virtual photon, and the cross sections of the processes can usually be expressed in terms of the electromagnetic transition form factors, or helicity transition amplitudes. Those functions depend on the four-momentum transfer squared  $q^2$ , and characterize the electromagnetic structure of such resonant states.

The data extracted from experiments in facilities such as Jefferson Lab (JLab) and MAMI (Mainz) allow us to extract the electromagnetic transition form factors of resonant states in the region  $Q^2 < 5 \text{ GeV}^2$  ( $Q^2 = -q^2$ ), corresponding to the first and second resonance region  $W < 1.6 \text{ GeV}$ , with  $W$  being the  $\gamma^*N$  invariant mass [1,2]. The planned JLab 12-GeV upgrade will enable us to make a detailed study of the resonances in the third-resonance region ( $W \approx 1.7 \text{ GeV}$ ) [2,3].

There has been some evidence of the existence of a state  $N(1710)$  with quantum numbers  $J^P = \frac{1}{2}^+$  since the 1980s [4,5]. [In the notation of the  $\pi N$  scattering it is labeled as  $N(1710)P_{11}$  [6].] The state  $N(1710)\frac{1}{2}^+$  is now classified as a three-star resonance, and found by several groups [7–15] in their partial wave analyses, and it is also included in some baryon-meson reaction models [16–22]. The resonance identified as  $N(1710)\frac{1}{2}^+$  has a small decay branching ratio for the  $\pi N$  channel, but significant decay branching ratios for the  $\eta N$ ,  $K\Lambda$  and  $\pi\pi N$  channels [6], and thus, may have important roles in kaon [23] and hypernuclear

production [24]. However, in some partial wave analyses like SAID (GWU), the resonance is not present [25]. Thus, the clear existence of the  $N(1710)$  state is still controversial, although some authors defend that it should be classified as a four-star resonance [9]. A state  $N\frac{1}{2}^+$  with a mass near  $1.7 \text{ GeV}$  collected also some interest as a possible partner of the  $\Theta^+$  pentaquark, nonstrange anti-decouplet state [26,27]. However, recent experimental evidence on the existence of the  $\Theta^+$  pentaquark seems to have been weakened [27]. Lattice QCD simulations predict also  $N\frac{1}{2}^+$  states that can possibly be related to the  $N(1710)$  state [28]. Future experiments, like the ones planned at the JLab 12-GeV upgraded facility, will help to establish or deny the existence of the  $N(1710)$  state. If the existence of the  $N(1710)$  state is confirmed, measurement of the  $\gamma^*N \rightarrow N(1710)$  helicity amplitudes will be possible. Thus, it is important to present predictions at this stage for the reaction associated with  $N(1710)$ , as we do in the present study.

In the usual nonrelativistic quark models the resonances  $N(1440)$  (also called Roper) and  $N(1710)$  can be classified as  $N\frac{1}{2}^+$  states with two different radial excitations of the nucleon, although the masses are different from the corresponding resonant poles [29,30]. The Roper has intriguing properties that are difficult to explain in the context of the quark model framework [1,2,29–33]. In a nonrelativistic quark model description the mass of the Roper is too heavy and the decay width is too narrow to be compatible with a three-quark ( $qqq$ ) system. Therefore, several alternative descriptions were suggested, e.g., by identifying the state as a quark bare core combined with gluon states ( $qqqG$ ), a molecular-type state ( $N\sigma$ ), or a dynamically generated state by baryon and meson. However, recent data from CLAS and MAID [34,35] for  $Q^2 > 2 \text{ GeV}^2$  support the assumption that the  $N(1440)$  is predominantly the first radial excitation of the nucleon [1]. Estimates made by constituent and light-front quark models

gave a good description for the high  $Q^2$  region data. For a review concerning the  $N(1440)$  resonance, see Ref. [1].

Based on the knowledge of the Roper, one can raise the following question, whether or not the  $N(1710)$  state can be described as another radial excitation of the nucleon. Some other works describe the state as a three-quark system [36–41], as a baryon bare core with a meson cloud [42], or  $\sigma$ -meson and glueball excitations [43]. There are, however, suggestions that the state  $N(1710)$  may be more likely generated dynamically by baryon-meson states [22,31,32,44]. The state  $N(1710)$  is also predicted in algebraic models of QCD [45,46] and in the large  $N_c$  limit [47]. The wave function of the  $N(1710)$  is also estimated by lattice QCD simulations [48].

As already recognized for the Roper and several other resonance cases, the meson cloud dressing for the transition helicity amplitudes is expected to be important only in the low  $Q^2$  region [1,2]. At high  $Q^2$  the valence quark degrees of freedom are expected to dominate and the helicity amplitudes follow the power laws,  $A_{1/2} \propto 1/Q^3$  and  $S_{1/2} \propto 1/Q^5$  [49]. In this work focusing on the high  $Q^2$  region, we predict the form factors and the helicity amplitudes of the  $\gamma^*N \rightarrow N(1710)$  reaction using a relativistic constituent quark model and the assumption that the  $N(1710)$  state is the second radial excitation of the nucleon state. That is our working hypothesis. In the near future our predictions can thus be indeed tested in the JLab 12-GeV upgraded facility.

In the previous works the nucleon and  $N(1440)$  structures were described in the covariant spectator quark model [50,51] as analogous states with different radial excitation. In there the  $N(1440)$  wave function was determined uniquely from the nucleon wave function by imposing that the  $N(1440)$  radial wave function is orthogonal to the nucleon radial wave function, without any new adjustable parameters in the model [51]. In the present work we extend the procedure to the second radial excitation of the nucleon (first radial excitation of the Roper),  $N(1710)$ . In a similar manner, the radial wave function of  $N(1710)$  can be determined by the two orthogonality conditions between the  $N(1710)$  radial wave function and both of the Roper and nucleon wave functions, again without any new adjustable parameters. The price we must pay for the present prediction is that the estimates of the electromagnetic properties are expected to be valid only in the high  $Q^2$  region, since the calculations are based exclusively on the valence quark degrees of freedom.

We will conclude that the transition helicity amplitudes for the  $\gamma^*N \rightarrow N(1710)$  reaction have their magnitude and falloff very similar to those for the  $\gamma^*N \rightarrow N(1440)$  reaction for  $Q^2 > 4 \text{ GeV}^2$ .

This article is organized as follows. In Sec. II we define the transition form factors and the helicity amplitudes. We describe in Sec. III the covariant spectator quark model, and present the baryon wave functions and the analytic expressions for the transition form factors and the helicity

amplitudes. The numerical results are presented in Sec. IV, and finally, the summary and the conclusions are given in Sec. V.

## II. ELECTROMAGNETIC FORM FACTORS AND HELICITY AMPLITUDES

The electromagnetic transition between a nucleon (mass  $M$ ) and a resonance  $N^*$  (mass  $M_R$ ) with  $J^P = \frac{1}{2}^+$  can be described by the current (in units of the proton charge  $e$ ) [1,51]

$$J^\mu = \left( \gamma^\mu - \frac{\not{q}\not{q}^\mu}{q^2} \right) F_1^*(Q^2) + \frac{i\sigma^{\mu\nu}q_\nu}{M_R + M} F_2^*(Q^2), \quad (2.1)$$

which defines the Dirac ( $F_1^*$ ) and Pauli ( $F_2^*$ ) form factors. The current operator  $J^\mu$  can be projected on the Dirac spinors of the resonance  $u_R(P_+)$  and of the nucleon  $u(P_-)$ , where  $P_+$  ( $P_-$ ) is the final (initial) momentum,  $q = P_+ - P_-$  and  $Q^2 = -q^2$ . Spin projection indices are suppressed in the spinors for simplicity.

The experimental data measured for hadron electromagnetic reactions are usually reported in terms of the helicity amplitudes in the final state ( $N^*$ ) rest frame. In this case the current (2.1) is projected on the initial and final spin states using the photon polarization states,  $\epsilon_\lambda^\mu$ , with  $\lambda = 0, \pm$  being the photon spin projection. In the  $N^*$  rest frame, one has the helicity amplitudes,  $A_{1/2}$  and  $S_{1/2}$ , which are given by [1,51]

$$A_{1/2}(Q^2) = \mathcal{K} \left\langle N^*, +\frac{1}{2} \left| \epsilon_+ \cdot J \right| N, -\frac{1}{2} \right\rangle, \quad (2.2)$$

$$S_{1/2}(Q^2) = \mathcal{K} \left\langle N^*, +\frac{1}{2} \left| \epsilon_0 \cdot J \right| N, +\frac{1}{2} \right\rangle \frac{|\mathbf{q}|}{Q}, \quad (2.3)$$

where

$$\mathcal{K} = \sqrt{\frac{2\pi\alpha}{K}}, \quad (2.4)$$

with  $\alpha = \frac{e^2}{4\pi} \simeq \frac{1}{137}$ ,  $K = \frac{M_R^2 - M^2}{2M_R}$ .  $|\mathbf{q}|$  is the photon momentum in the  $N^*$  rest frame,

$$|\mathbf{q}| = \frac{\sqrt{Q_+^2 - Q_-^2}}{2M_R}, \quad (2.5)$$

where  $Q_\pm^2 = (M_R \pm M)^2 + Q^2$ .

The helicity amplitudes  $A_{1/2}$  and  $S_{1/2}$  can be related with the form factors  $F_1^*$  and  $F_2^*$  via Eqs. (2.1)–(2.3) [1,51] as

$$A_{1/2}(Q^2) = \mathcal{R} \{ F_1^*(Q^2) + F_2^*(Q^2) \}, \quad (2.6)$$

$$S_{1/2}(Q^2) = \frac{\mathcal{R}}{\sqrt{2}} |\mathbf{q}| \frac{M_R + M}{Q^2} \{ F_1^*(Q^2) - \tau F_2^*(Q^2) \}, \quad (2.7)$$

where  $\tau = \frac{Q^2}{(M_R+M)^2}$ , and

$$\mathcal{R} = \frac{e}{2} \sqrt{\frac{Q_-^2}{M_R M K}}. \quad (2.8)$$

Note that the amplitude  $S_{1/2}$  is determined by the virtual photons and not specified at  $Q^2 = 0$ . The analytic properties of the current (2.1) imply that  $F_1^*(0) = 0$  [51].

### III. COVARIANT SPECTATOR QUARK MODEL

The covariant spectator quark model is derived from the formalism of the covariant spectator theory [52]. In the model a baryon  $B$  is described as a three-constituent-quark system, where one quark is free to interact with the electromagnetic fields and the other quarks are on mass shell. Integrating over the on-mass-shell momenta, one can represent the quark pair as an on-mass-shell diquark with effective mass  $m_D$ , and the baryon as a quark-diquark system [2,50,53,54]. The structure of the baryon is then described by a transition vertex between the three-quark bound state and a quark-diquark state that describes effectively the confinement [50,54].

The baryon wave function  $\Psi_B(P, k)$  is then derived from the transition vertex as a function of the baryon momentum  $P$  and the diquark momentum  $k$  taking into account the properties of the baryon  $B$ , such as the spin and flavor. Instead of solving dynamical equations to get wave functions, the wave functions  $\Psi_B$  are built from the baryon internal symmetries, with the shape determined directly by experimental or lattice data for some ground state systems [2,50,55,56]. The baryon mass  $M_B$  is a parameter fixed by the experimental value. In particular the parametrization of the nucleon wave function was calibrated by the nucleon electromagnetic form factor data [50].

In the past the covariant spectator quark model was applied to several nucleon resonances such as  $N(1520)$  [57],  $N(1535)$  [58],  $\Delta$  resonances [55,56,59–61], and also to other reactions [54,62–64].

#### A. Transition current

Once the baryon wave functions are written in terms of the single quark and quark-pair states, one can write the transition current between the baryons  $B$  and  $B'$  in a relativistic impulse approximation as [50,53,54]

$$J_{B'B}^\mu = 3 \sum_{\Gamma} \int_k \bar{\Psi}_{B'}(P_+, k) j_q^\mu \Psi_B(P_-, k), \quad (3.1)$$

where  $j_q^\mu$  is the (single) quark current operator,  $P_-$  ( $P_+$ ) is the initial (final) momentum, and  $\Gamma$  labels the scalar diquark and vectorial diquark (projections  $\Lambda = 0, \pm$ ) polarizations. The factor 3 takes account of the contributions from the other quark pairs by the symmetry, and the integration symbol represents the covariant integration for the

diquark on-mass-shell state  $\int_k \equiv \int \frac{d^3\mathbf{k}}{(2\pi)^3(2E_D)}$ , with  $E_D = \sqrt{m_D^2 + \mathbf{k}^2}$ . Compared to Eq. (2.1), the current  $J^\mu$  is in this case projected on the initial and final states, and labeled respectively by the indices  $B$  and  $B'$ .

The quark current operator is expressed in terms of the Dirac ( $j_1$ ) and Pauli ( $j_2$ ) quark form factors [50,54]:

$$j_q^\mu = j_1(Q^2) \left( \gamma^\mu - \frac{\not{q} q^\mu}{q^2} \right) + j_2(Q^2) \frac{i\sigma^{\mu\nu} q_\nu}{2M}. \quad (3.2)$$

The inclusion of the terms  $-\frac{\not{q} q^\mu}{q^2}$  associated with the Dirac component is equivalent with using the Landau prescription for the current  $J_{B'B}^\mu$  [65,66]. This term restores current conservation, but does not affect the results for the observables [65]. For the case where the baryons are composed only of  $u$  and  $d$  quarks, the quark form factors  $j_i$  ( $i = 1, 2$ ) can be decomposed into an isoscalar and an isovector component given respectively by the functions  $f_{i+}$  and  $f_{i-}$ :

$$j_i = \frac{1}{6} f_{i+}(Q^2) + \frac{1}{6} f_{i-}(Q^2) \tau_3. \quad (3.3)$$

The quark form factors are parametrized based on the vector meson dominance mechanism [50,54,60,62]. The functions  $f_{i\pm}$  are constrained at  $Q^2 = 0$  in order to reproduce the quark charges and so as to properly parametrize the anomalous magnetic moments of the constituent quarks. The details are given in the Appendix.

#### B. Baryon wave functions

Next, we discuss the wave functions of the nucleon and the nucleon radial excited states,  $N(1440)$  and  $N(1710)$ , which will respectively be denoted by  $N0, N1$  and  $N2$ . In the covariant spectator quark model the nucleon and its radial excitation can be described as a quark-diquark system in an  $S$ -state configuration [50]. Following Refs. [50,51], we can represent the  $N_j$  ( $j = 0, 1, 2$ ) wave functions as

$$\Psi_{N_j}(P, k) = \frac{1}{\sqrt{2}} [\phi_I^0 \phi_S^0 + \phi_I^1 \phi_S^1] \psi_{N_j}(P, k), \quad (3.4)$$

where  $\phi_S^{0,1}$  and  $\phi_I^{0,1}$  represent respectively the spin ( $S$ ) and isospin ( $I$ ) states corresponding to the total magnitude of either 0 or 1 in the diquark configuration [50]. (See the Appendix for details.) Again, we suppress the spin and isospin projection indices for simplicity. The wave function represented by Eq. (3.4) satisfies the Dirac equation [50,55]. The functions  $\psi_{N_j}(P, k)$  are the radial wave functions to be described next.

The radial wave functions  $\psi_{N_j}$  depend on the angular momentum and the radial excitation of the baryons. Since the baryon and the diquark are both on mass shell, one can

write the radial wave functions  $\psi_{Nj}$  for the quark-diquark system as a function of  $(P-k)^2$  (or  $P \cdot k$ ) [50]. To take into account the dependence on a generic baryon  $B$ , or its mass  $M_B$ , one can use the dimensionless variable:

$$\chi_B = \frac{(M_B - m_D)^2 - (P-k)^2}{M_B m_D}. \quad (3.5)$$

In the present study  $B = N0, N1$  or  $N2$ . For the nucleon mass ( $M_{N0}$ ) we also use  $M$  for simplicity.

For the nucleon radial wave function, we use [50]

$$\psi_{N0}(\chi_N) = N_0 \frac{1}{m_D(\beta_1 + \chi_N)(\beta_2 + \chi_N)}, \quad (3.6)$$

where  $N_0$  is the normalization constant, and the parameter values are  $\beta_1 = 0.049$  and  $\beta_2 = 0.717$ , which were determined by the fit to the nucleon electromagnetic form factors [50]. If we choose the momentum-range parameters such that  $\beta_1 < \beta_2$ ,  $\beta_1$  regulates the spacial long-range structure.

For the Roper ( $N1$ ), we take the form [51]

$$\psi_{N1}(\chi_{N1}) = N_1 \frac{\beta_3 - \chi_{N1}}{\beta_1 + \chi_{N1}} \frac{1}{m_D(\beta_1 + \chi_{N1})(\beta_2 + \chi_{N1})}, \quad (3.7)$$

where  $N_1$  is the normalization constant, and  $\beta_3$  is a new parameter fixed by the orthogonality condition with the nucleon state. As explained in Ref. [51], the term  $(\beta_3 - \chi_{N1})$  represents the radial excitation in the momentum space [term on  $(P-k)^2$  or  $\chi_{N1}$ ].

Finally for the  $N(1710)$  ( $N2$ ), we define the radial wave function as

$$\psi_{N2}(\chi_{N2}) = N_2 \frac{\chi_{N2}^2 - \beta_4 \chi_{N2} + \beta_5}{(\beta_1 + \chi_{N2})^2} \times \frac{1}{m_D(\beta_1 + \chi_{N2})(\beta_2 + \chi_{N2})}, \quad (3.8)$$

where  $N_2$  is the normalization constant. In this case we have two additional parameters  $\beta_4$  and  $\beta_5$  to be fixed. The minus sign in the coefficient  $\beta_4$  is introduced by convenience.

In our model the sign of the normalization constants  $N_l$  ( $l = 0, 1, 2$ ) cannot be predicted. In the previous works [50,51] the relative sign of  $N_0$  and  $N_1$  was determined by the sign of the form factors. In the present case since there are no available data for the high  $Q^2$  region, we have no way of fixing the sign of  $N_2$  based on an experimental basis. We assume here that  $N_2$  is positive. If future experimental data reveal an opposite sign, we should correct the signs of the corresponding amplitudes.

The normalization of the radial wave functions  $\psi_{Nj}$  is determined by the normalization of the wave function (3.4) in order to obtain the corresponding charge of the state. The explicit expression is

$$\sum_{\Gamma} \int_k \bar{\Psi}_{Nj}(\bar{P}, k) j_1 \gamma^0 \Psi_{Nj}(\bar{P}, k) = \frac{1}{2} (1 + \tau_3) \int_k |\psi_{Nj}(\bar{P}, k)|^2. \quad (3.9)$$

In the above  $\bar{P}$  is the baryon momentum at its rest frame;  $j_1 = \frac{1}{6} + \frac{1}{2} \tau_3$  is the quark charge operator in the  $Q^2 = 0$  limit. In order to obtain the baryon charge  $\frac{1}{2} (1 + \tau_3)$  correctly, we need the normalization condition,

$$\int_k |\psi_{Nj}(\bar{P}, k)|^2 = 1. \quad (3.10)$$

The orthogonality among the  $N0$ ,  $N1$  and  $N2$  states is derived from

$$\sum_{\Gamma} \int_k \bar{\Psi}_{Nj'}(\bar{P}_+, k) j_1 \gamma^0 \Psi_{Nj}(\bar{P}_-, k) = 0, \quad (3.11)$$

where  $\bar{P}_+$  and  $\bar{P}_-$  are the momenta of  $Nj'$  and  $Nj$  respectively, for  $Q^2 = 0$ .

### C. Valence quark contributions for the electromagnetic form factors

In order to write the expressions for the form factors, it is convenient to project the quark current  $j_i$  on the isospin states using  $j_i^A = (\phi_l^0)^\dagger j_i \phi_l^0$ , and  $j_i^S = (\phi_l^1)^\dagger j_i \phi_l^1$ :

$$j_i^A = \frac{1}{6} f_{i+} + \frac{1}{2} f_{i-} \tau_3, \quad (3.12)$$

$$j_i^S = \frac{1}{6} f_{i+} - \frac{1}{6} f_{i-} \tau_3. \quad (3.13)$$

The results for the form factors are then given by

$$F_1^*(Q^2) = \left[ \frac{3}{2} j_1^A + \frac{1}{2} \frac{3 - \tau}{1 + \tau} j_1^S - 2 \frac{\tau}{1 + \tau} \frac{M_{N2} + M}{2M} j_2^S \right] \mathcal{I}(Q^2), \quad (3.14)$$

$$F_2^*(Q^2) = \left[ \left( \frac{3}{2} j_2^A - \frac{11 - 3\tau}{2} \frac{1}{1 + \tau} j_2^S \right) \frac{M_{N2} + M}{2M} - 2 \frac{1}{1 + \tau} j_1^S \right] \mathcal{I}(Q^2), \quad (3.15)$$

with  $\tau = \frac{Q^2}{(M_{N2} + M)^2}$ , and

$$\mathcal{I}(Q^2) = \int_k \psi_{N2}(P_+, k) \psi_{N0}(P_-, k) \quad (3.16)$$

is the overlap integral between the initial and final radial wave functions. The integral  $\mathcal{I}$  is frame independent and is discussed in the next section.

Equations (3.14) and (3.15) are equivalent to the ones presented in the study of  $\gamma^* N \rightarrow N(1440)$  [51], although



they are shown in different forms. The analytic expressions obtained for  $F_1^*$  and  $F_2^*$  are consistent with the results obtained for other systems with the same spin structure [50,62]. If we replace  $\psi_{N2} \rightarrow \psi_N$  and  $M_{N2} + M \rightarrow 2M$ , we recover the expressions for the nucleon elastic form factors [50]. The expressions can also be related with the octet baryon elastic form factors. Except for the fact that  $j_i^A$  and  $j_i^S$  can depend also on the strange quark, the expressions are the same when replacing  $\psi_{N2}, \psi_N \rightarrow \psi_B$  and  $M_{N2} + M \rightarrow 2M_B$ , with  $\psi_B$  and  $M_B$  being the octet baryon radial wave functions and their masses respectively [62].

#### D. Orthogonality between the states

The consequence of the condition (3.11) is that the orthogonality between the states is replaced by the condition for the radial wave functions [51]

$$\int_k \psi_{Nj'}(\bar{P}_+, k) \psi_{Nj}(\bar{P}_-, k) = 0, \quad (3.17)$$

where we recall that  $\bar{P}_\pm$  are the momenta for the case  $Q^2 = 0$ .<sup>1</sup>

Since the zero overlap between the radial wave functions is equivalent to the orthogonality between the radial wave functions due to Eq. (3.17), to discuss how the orthogonality is assured, and how the parameters of the wave functions  $\psi_{N1}$  and  $\psi_{N2}$  given by Eqs. (3.7) and (3.8) are determined, we define the integral function:

$$\mathcal{I}_{j'j}(Q^2) = \int_k \psi_{Nj'}(P_+, k) \psi_{Nj}(P_-, k). \quad (3.18)$$

Note that with the above notation one has from Eq. (3.16):  $\mathcal{I}(Q^2) \equiv \mathcal{I}_{20}(Q^2)$ . As for  $\mathcal{I}$ , the integrals  $\mathcal{I}_{j'j}$  are covariant and frame independent. In the following we will consider only the case  $Q^2 = 0$ .

The orthogonality between  $N1$  and  $N0$  can be imposed by the condition  $\mathcal{I}_{10}(0) = 0$ , which can be used to calculate the value of  $\beta_3$ . The result obtained by this condition is  $\beta_3 = 0.1300$  [51].

We discuss now the orthogonality between the  $N2$  and the other states,  $N1$  and  $N0$ . Using the notation of Eq. (3.18), we can write the orthogonality with  $N0$  and  $N1$  by the two conditions:

<sup>1</sup>Considering for instance the rest frame of the final state for  $Q^2 = 0$ , one has

$$\bar{P}_+ = (M_{Nj'}, 0, 0, 0), \bar{P}_- = \left( \frac{M_{Nj'}^2 + M_{Nj}^2}{2M_{Nj'}}, 0, 0, -\frac{M_{Nj'}^2 - M_{Nj}^2}{2M_{Nj'}} \right)$$

defining the three-momentum along  $z$ . The sign of the  $z$  component is chosen in order to obtain  $q$  with a positive sign along with the  $z$  axis.

$$\mathcal{I}_{20}(0) = 0, \quad \mathcal{I}_{21}(0) = 0. \quad (3.19)$$

Choosing proper frames for each integral, we can reduce Eqs. (3.19) to a system of two equations with two unknowns,  $\beta_4$  and  $\beta_5$ . The results obtained by solving the set of the two equations are  $\beta_4 = 0.3377$  and  $\beta_5 = 0.00855$ .

#### IV. RESULTS

In the present work we consider only the reaction with the proton ( $N = p$ ), since there are no data for the neutron ( $N = n$ ) for finite  $Q^2$ , and our model is expected to work better in the region of large  $Q^2$ . The results for the form factors are presented in Fig. 1, and those for the helicity amplitudes are presented in Fig. 2, both up to  $Q^2 = 12 \text{ GeV}^2$ .

In Fig. 1, we also include the results for  $\gamma^*N \rightarrow N(1440)$  obtained in Ref. [51]. From Fig. 1, it is clear that both reactions yield very close results for the form factors  $F_1^*$  and  $F_2^*$ , in the region  $Q^2 > 2 \text{ GeV}^2$ . Recall that it is in the high  $Q^2$  region that our model is more reliable, since the valence quark degrees of freedom are expected to be dominant. In Fig. 1 we also include the experimental data for the  $\gamma^*N \rightarrow N(1440)$  reaction from CLAS for comparison (data set with the highest value for  $Q^2$ ). It is appreciable from Fig. 1 that the agreement of the model (dashed line) and the data is very good for the higher  $Q^2$  region ( $Q^2 > 2 \text{ GeV}^2$ ). Only for the last  $Q^2$  data point we can observe for  $F_2^*$  a

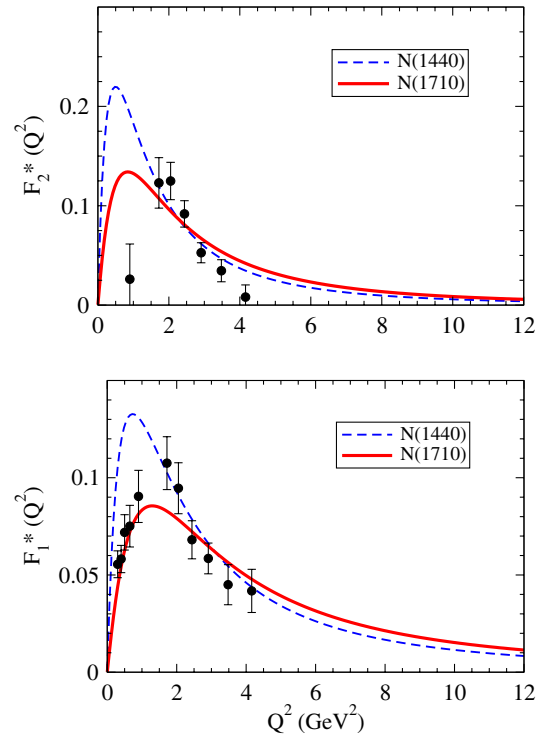


FIG. 1 (color online).  $\gamma^*N \rightarrow N(1710)$  transition form factors (solid line) compared with those for the Roper,  $\gamma^*N \rightarrow N(1440)$  (dashed line). Data for the Roper are from CLAS [34].

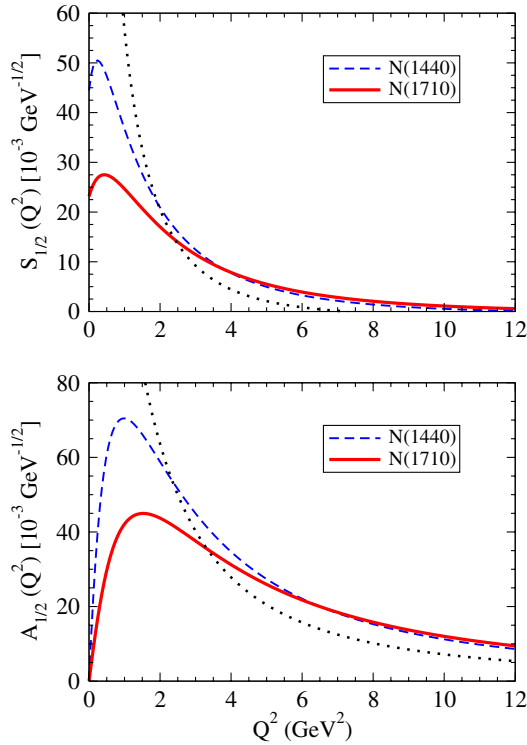


FIG. 2 (color online).  $\gamma^*N \rightarrow N(1710)$  helicity amplitudes at the resonance rest frame (solid line). Results are compared with those for the  $\gamma^*N \rightarrow N(1440)$  amplitudes (dashed line), and the *equivalent* amplitude for the nucleon  $N(939)$  (dotted line). See the text for the explanation on the *equivalent* nucleon case.

larger difference, about 2 standard deviations, between the model result and the data. New data for the higher  $Q^2$  region are necessary to test the model in more detail. Other data sets are not included since they are restricted to the low  $Q^2$  region, the region dominated by the meson cloud effects, and therefore we should expect deviations from our results [1,51,67].

The results for the amplitudes in Fig. 2 are calculated using the form factors given in Eqs. (2.6) and (2.7) for both cases,  $N(1440)$  and  $N(1710)$ . The Particle Data Group (PDG) result for the  $N(1710)$  case  $A_{1/2}(0) = (24 \pm 10) \times 10^{-3} \text{ GeV}^{-1/2}$  [6] is not included, since we are focusing on the larger  $Q^2$  region. Note that the amplitudes for the two reactions are even closer than the results for the form factors, particularly for  $Q^2 > 4 \text{ GeV}^2$ .

It is possible that the closeness of the results for these reactions in the higher  $Q^2$  region is a consequence of the forms of the radial wave functions (3.6)–(3.8), where the radial wave functions of the excited states are related with the ground state nucleon radial wave function. Note that all the radial wave functions are parametrized with the same short-range structure given by the factor  $1/(\beta_2 + \chi)$ , apart from the mass differences in  $\chi$ . Since the coupling with the photon with high  $Q^2$  probes the short-range structure of the baryon states it is expected that the form factors at high  $Q^2$

have the same shape since they are described by the same parametrization.

In order to examine the above arguments in more detail, we plot also the *equivalent* results for the nucleon case (dotted line). Note that, according to Eqs. (2.6) and (2.7) the amplitudes for the nucleon are proportional to  $G_M(A_{1/2})$  and  $G_E(S_{1/2})$ , but also there is an extra factor  $\mathcal{R}$  depending on  $K = \frac{M_R^2 - M^2}{2M_R}$ , that vanishes and induces singularities in the amplitudes in the elastic limit ( $M_R = M$ ). In order to be able to compare the results of the nucleon with those of the  $N(1440)$  and  $N(1710)$ , we keep the expression of  $\mathcal{R}$  given for the  $N(1440)$  and take the  $M_R \rightarrow M$  limit in the factor  $|\mathbf{q}| \frac{M_R + M}{Q^2}$ , giving  $\sqrt{\frac{1+\epsilon}{\tau}}$ , in the case of  $S_{1/2}$ . From Fig. 2 we can see that, apart from the magnitude (about  $1/\sqrt{2}$  smaller), the falloffs of the nucleon *equivalent* amplitudes are about the same as those of the  $N(1440)$  and  $N(1710)$ .

### A. High $Q^2$ parametrization

To make a comparison easier with the expected future experimental data, we parametrize our model results using the simple analytic form,

$$A_{1/2} = A \left( \frac{\Lambda_1^2}{\Lambda_1^2 + Q^2} \right)^{3/2}, \quad (4.1)$$

$$S_{1/2} = S \left( \frac{\Lambda_2^2}{\Lambda_2^2 + Q^2} \right)^{5/2}, \quad (4.2)$$

which is consistent with the falloff expected for very large  $Q^2$  [49]. In Eqs. (4.1) and (4.2),  $A$  and  $S$  are constants, and  $\Lambda_1^2$  and  $\Lambda_2^2$  are cutoffs squared.

The numerical values for the parametrization are given in Table I. The parameters are determined so as to reproduce the results exactly at  $Q^2 = 6 \text{ GeV}^2$ , but provide also good approximations for the values of  $Q^2$  up to  $10 \text{ GeV}^2$ . The exception is the parametrization for the amplitude  $S_{1/2}$  in the  $\gamma^*N \rightarrow N(1440)$  reaction that approaches zero very fast. In this case the approximation is valid only around  $Q^2 = 5 \text{ GeV}^2$ , and thus the respective parameters in Table I are written in *italic*. Note that the expressions (4.1) and (4.2) are only valid in the range of  $Q^2$  presented in the figures. In general the covariant spectator quark model has smooth logarithmic corrections for the form factors and helicity amplitudes [50,51]. Therefore the parametrizations

TABLE I. Parametrization for the helicity amplitudes for the higher  $Q^2$  region according to Eqs. (4.1) and (4.2). See discussion in the main text.

	$A(10^{-3} \text{ GeV}^{-1/2})$	$\Lambda_1^2(\text{GeV}^2)$	$S(10^{-3} \text{ GeV}^{-1/2})$	$\Lambda_2^2(\text{GeV}^2)$
$N(1440)$	275.40	1.374	<i>727.53</i>	<i>0.789</i>
$N(1710)$	122.17	2.783	210.71	1.531

given by Eqs. (4.1) and (4.2) and Table I are not valid for an arbitrary high  $Q^2$ .

Since our results for the form factors are well approximated by the parametrizations (4.1) and (4.2) for the region 5–10 GeV<sup>2</sup>, we can expect evidences of asymptotic behavior for  $Q^2 > 5$  GeV<sup>2</sup>.

### B. Discussion of results

The  $\gamma^*N \rightarrow N(1710)$  reaction was studied in the past within several frameworks. We start discussing the results from quark models, and later discuss other models.

Analytic expressions for the  $\gamma^*N \rightarrow N(1710)$  helicity amplitudes derived from an algebraic model of QCD, also based on the quark degrees of freedom, can be found in Ref. [45]. Estimates from quark models are given in Refs. [37,40,41]. The magnitudes of those estimates are consistent with our predictions. In general the amplitudes  $A_{1/2}$  and  $S_{1/2}$  are positive. The exception is Ref. [40], where  $S_{1/2}$  is negative.

Some other models describe the  $N(1710)$  state as a quark bare core with some excitations [42,43]. In Ref. [42] a coupled-channel formalism is combined with a description of the baryon bare cores and meson production based on the cloudy bag model. In Ref. [43] the  $N(1710)$  state is described by a baryon bare core with some radial excitations combined with glueball and  $\sigma$  vibrational excitations. In both cases [42,43], we can expect a dominance of the bare core in the high  $Q^2$  region, since the meson cloud is expected to be suppressed.

In other frameworks the  $N(1710)$  state is dynamically generated from some baryon and meson states [22,31,32,44].

The EBAC model [31,32] uses baryon-meson coupled-channel formalism to describe the photo- and electroproduction of mesons by nucleons. In that framework the  $N(1710)$  identified as  $N(1820)$  is a state that evolves from an  $N(1763)$  bare core state through its coupling with the  $\pi N$ ,  $\eta N$  and  $\pi\pi N$  channels. The EBAC model is also used to extract the amplitude  $A_{1/2}$  from the data, for  $Q^2 < 1.5$  GeV<sup>2</sup> in Ref. [32]. Although their results cannot be compared with our results which are reliable only for the high  $Q^2$  region, we note that the real part of the amplitude they extracted is positive, with the magnitude comparable with ours.

In Ref. [22] by solving the Faddeev equations with the input of the two-body coupled-channel  $t$  matrices, the  $N(1710)$  state is explained as a dynamical generated resonance dominated by the  $\pi\pi N$  component (the  $\pi\pi$  component can be also interpreted as a  $\sigma$  meson). Also in Ref. [44] the  $N(1710)$  emerges as the result of the pion dressing of nucleon and  $\Delta$  bare cores. The model parameters were fixed to reproduce masses and branching ratios.

In models that the  $N(1710)$  state is generated by the baryon-meson interactions as the ones mentioned above [22,31,32,44], we can expect a much larger spatial extended structure for  $N(1710)$ , and consequently a faster falloff with  $Q^2$  for the associated transition amplitudes [46].

From the discussions above, we conclude that we can deduce the nature of the  $N(1710)$  state by the  $Q^2$  behavior of the helicity amplitudes, which may be revealed in future experiments. Assuming a dominance of the valence quark effects as we do, we expect  $A_{1/2} \propto 1/Q^3$  and  $S_{1/2} \propto 1/Q^5$  in the very large  $Q^2$  region. Instead, if the  $N(1710)$  system is dominated by  $qqq$ -( $q\bar{q}$ ) configurations, the falloffs mentioned previously are modified by an extra  $1/Q^4$  factor according to perturbative QCD [49].

A few words are in order on the possible existence of another  $N_{\frac{1}{2}}^{1+}$  state with an invariant mass near 1.7 GeV. PDG reports a fourth  $N_{\frac{1}{2}}^{1+}$  state (two-star resonance) denoted by  $N(1880)$ . However, several partial wave analyses and coupled-channel reaction models suggest the existence of another  $N_{\frac{1}{2}}^{1+}$  state near the mass 1.7 GeV. See for instance Refs. [9–11,14,18,21]. If there exist two  $N_{\frac{1}{2}}^{1+}$  states with very close masses around 1.7 GeV, the experimental determination of the individual contributions will be very difficult. Then, the transition helicity amplitudes extracted from the data would be a combination of the two resonances, and our model, that assumes only one radial excited state, would fail the description of the data.

### V. SUMMARY AND CONCLUSIONS

The future JLab 12-GeV facility will open a possibility of studying in detail the electromagnetic structure of the resonances in the third-resonance region. There is then the chance of exploring the resonances  $N(1720)_{\frac{3}{2}}^{3+}$ ,  $\Delta(1720)_{\frac{3}{2}}^{3-}$  (four-star resonances),  $N(1710)_{\frac{1}{2}}^{1+}$  and  $N(1700)_{\frac{3}{2}}^{3-}$  (three-star resonances). Among these the  $N(1710)_{\frac{1}{2}}^{1+}$  is a very interesting system due to the significant branching ratios to the  $\eta N$ ,  $K\Lambda$  and  $\pi\pi N$  channels. Some authors defend even that the state should be reclassified as a four-star resonance [9].

Future data for the invariant mass  $W \approx 1.7$  GeV will help to clarify the nature of the state  $N(1710)_{\frac{1}{2}}^{1+}$ , namely, if it is a radial excitation of the nucleon and the Roper, or a more complex and/or exotic system. From the observation of the measured helicity amplitudes in the large  $Q^2$  region, we will be able to draw some conclusion on the dominant degrees of freedom in the system at large  $Q^2$ . If  $N(1710)$  is dominated by the valence quark degrees of freedom only, we should observe the scaling behavior with  $Q^2$  as  $A_{1/2} \propto 1/Q^3$ . In the case of baryon-meson *molecular* system we expect a falloff of  $A_{1/2}$  faster than  $1/Q^3$ . In addition, in principle it will also be possible to answer the question if there is another  $N_{\frac{1}{2}}^{1+}$  state close to the one that we study in this work.

In this work we have used the covariant spectator quark model to predict the transition form factors and the helicity amplitudes for the  $\gamma^*N \rightarrow N(1710)$  reaction. The covariant spectator quark model was already applied to several nucleon resonances successfully. Since we have not included the meson cloud effects which are known to be

very important in the low  $Q^2$  region, we expect our prediction to the  $\gamma^*N \rightarrow N(1710)$  helicity amplitudes to be valid only in the high  $Q^2$  region, where the valence quark degrees of freedom are dominant.

We have assumed that the  $N(1710)$  state is the second radial excitation of the nucleon, similar to the assumption that the Roper is the first radial excitation of the nucleon. The wave function of the  $N(1710)$  has been uniquely determined, apart from the sign, by the orthogonality of the  $N(1710)$  wave function with the nucleon and  $N(1440)$  wave functions. The nucleon and  $N(1440)$  wave functions were determined in the previous works [50,51].

For high  $Q^2$ , particularly for  $Q^2 > 4 \text{ GeV}^2$ , the calculated helicity amplitudes for the  $\gamma^*N \rightarrow N(1710)$  reaction have shown results that are very close to those for the  $\gamma^*N \rightarrow N(1440)$  reaction. Therefore, the future measurements of the helicity amplitudes in the large  $Q^2$  region can be used to test the assumption that the  $N(1710)$  state is the second radial excitation of the nucleon.

Finally we note that the present formalism can be used to study the radial excited states in the  $\Delta$  sector (isospin 3/2) [61], and also in the strange baryon sector. In the latter case we can study the transitions  $\gamma^*\Lambda \rightarrow \Lambda(1600)_{\frac{1}{2}}^{1+}$ ,  $\gamma^*\Lambda \rightarrow \Lambda(1810)_{\frac{1}{2}}^{1+}$  and  $\gamma^*\Sigma \rightarrow \Sigma(1660)_{\frac{1}{2}}^{1+}$  (all three-star resonances). More experimental support is necessary also in these cases.

## ACKNOWLEDGMENTS

The authors would like to thank Ralf Gothe and Catarina Quintans for helpful discussions. This work was supported by the Brazilian Ministry of Science, Technology and Innovation (MCTI-Brazil), and Conselho Nacional de Desenvolvimento Científico e Tecnológico (CNPq), Project No. 550026/2011-8.

## APPENDIX: COVARIANT SPECTATOR QUARK MODEL

In the following we present some details of the covariant spectator quark model.

### 1. Quark form factors

The quark current associated with Eq. (3.3) is expressed in terms of the quark form factors  $f_{i\pm}$  ( $i = 1, 2$ ) inspired by a vector meson dominance form:

$$f_{1\pm}(Q^2) = \lambda_q + (1 - \lambda_q) \frac{m_v^2}{m_v^2 + Q^2} + c_{\pm} \frac{M_h^2 Q^2}{(M_h^2 + Q^2)^2}, \quad (\text{A1})$$

$$f_{2\pm}(Q^2) = \kappa_{\pm} \left\{ d_{\pm} \frac{m_v^2}{m_v^2 + Q^2} + (1 - d_{\pm}) \frac{M_h^2}{M_h^2 + Q^2} \right\}. \quad (\text{A2})$$

In the above,  $\lambda_q$  defines the quark charge in deep inelastic scattering;  $\kappa_{\pm}$  are the isoscalar and isovector quark anomalous magnetic moments. The mass  $m_v$  ( $M_h$ ) corresponds to

TABLE II. Parameters in the quark current.

$\kappa_+$	$\kappa_-$	$c_+$	$c_-$	$d_+$	$d_-$	$\lambda_q$
1.639	1.823	4.16	1.16	-0.686	-0.686	1.21

the light (heavy) vector meson, and  $c_{\pm}$ ,  $d_{\pm}$  are the mixture coefficients. In the present model we set  $m_v = m_{\rho}$  ( $\approx m_{\omega}$ ) for the light vectorial meson and  $M_h = 2M$  (twice the nucleon mass) to represent the short-range physics. The values of the parameters were previously fixed by the nucleon elastic form factors [50], and they are presented in Table II. Note that the present model uses  $d_+ = d_-$ .

### 2. Wave functions

In the covariant spectator quark model the  $S$ -state wave functions for the nucleon and the nucleon radial excitations  $\Psi_{Nj}(P, k)$  can be represented by Eq. (3.4) for the states labeled by  $Nj$  with  $j = 0, 1, 2$  [50,51,62]. In Eq. (3.4) the isospin operators  $\phi_I^{0,1}$  act on the  $Nj$ 's isospin states  $\chi^t$ , where  $\chi^{+1/2} = (1 \ 0)^T$  and  $\chi^{-1/2} = (0 \ 1)^T$ . The explicit forms are [50,53]

$$\phi_I^0 \chi^t = \mathbb{1} \chi^t, \quad (\phi_I^1)_i \chi^t = -\frac{1}{\sqrt{3}} (\tau \cdot \xi_i^*) \chi^t, \quad (\text{A3})$$

where  $\xi_i$  is the isospin vector of the isospin-one diquark defined in a usual way (in the spherical basis),

$$\xi_{\pm} = \mp \frac{1}{\sqrt{2}} \begin{pmatrix} 1 \\ \pm i \\ 0 \end{pmatrix}, \quad \xi_0 = \begin{pmatrix} 0 \\ 0 \\ 1 \end{pmatrix}. \quad (\text{A4})$$

As for the spin states  $\phi_S^{0,1}$ , we start to present the spin-1 polarization vector  $\varepsilon_{\Lambda P}$  in a fixed-axis base for the case of a baryon with momentum  $P = (E_B, 0, 0, P_z)$ , where  $E_B = \sqrt{M_B^2 + P_z^2}$  [53,68]:

$$\varepsilon_{\pm P}^{\alpha} = \mp \frac{1}{\sqrt{2}} (0, 1, \pm i, 0), \quad \varepsilon_{0P}^{\alpha} = \left( \frac{P_z}{M_B}, 0, 0, \frac{E_B}{M_B} \right). \quad (\text{A5})$$

We can then write

$$\phi_I^0 = u_B(P), \quad \phi_I^1 = -(\varepsilon_{\Lambda P}^*)_{\alpha} U_B^{\alpha}(P), \quad (\text{A6})$$

where  $u_B$  is a Dirac spinor, and [55]

$$U_B^{\alpha}(P) = \frac{1}{\sqrt{3}} \gamma_5 \left( \gamma^{\alpha} - \frac{P^{\alpha}}{M_B} \right) u_B(P). \quad (\text{A7})$$

In the case of the nucleon one may replace  $u_B \rightarrow u$  and  $M_B \rightarrow M$ . In the case of a resonance  $R$  one may replace the index  $B$  by the index  $R$ .



- [1] I. G. Aznauryan and V. D. Burkert, *Prog. Part. Nucl. Phys.* **67**, 1 (2012).
- [2] I. G. Aznauryan, A. Bashir, V. Braun, S. J. Brodsky, V. D. Burkert, L. Chang, C. Chen, B. El-Bennich *et al.*, *Int. J. Mod. Phys. E* **22**, 1330015 (2013).
- [3] I. Aznauryan, V. Braun, V. Burkert, S. Capstick, R. Edwards, I. C. Cloet, M. Giannini, T. S. H. Lee *et al.*, [arXiv:0907.1901](https://arxiv.org/abs/0907.1901).
- [4] R. E. Cutkosky, C. P. Forsyth, R. E. Hendrick, and R. L. Kelly, *Phys. Rev. D* **20**, 2839 (1979).
- [5] G. Hohler and H. Schopper, in *Landolt-Börnstein: Numerical Data and Functional Relationships in Science and Technology*, edited by W. Martienssen (Springer-Verlag, Berlin, 1982), p. 407.
- [6] J. Beringer *et al.* (Particle Data Group), *Phys. Rev. D* **86**, 010001 (2012).
- [7] A. V. Anisovich, R. Beck, E. Klempt, V. A. Nikonov, A. V. Sarantsev, and U. Thoma, *Eur. Phys. J. A* **48**, 15 (2012).
- [8] M. Shrestha and D. M. Manley, *Phys. Rev. C* **86**, 055203 (2012).
- [9] S. Ceci, A. Svarc, and B. Zauner, *Phys. Rev. Lett.* **97**, 062002 (2006).
- [10] S. Ceci, A. Svarc, and B. Zauner, *Few-Body Syst.* **39**, 27 (2006).
- [11] H. Osmanovic, S. Ceci, A. Svarc, M. Hadzimehmedovic, and J. Stahov, *Phys. Rev. C* **84**, 035205 (2011).
- [12] V. Shklyar, H. Lenske, and U. Mosel, *Phys. Lett. B* **650**, 172 (2007).
- [13] W.-T. Chiang, S.-N. Yang, L. Tiator, and D. Drechsel, *Nucl. Phys. A* **700**, 429 (2002).
- [14] M. Batinic, I. Slaus, A. Svarc, and B. M. K. Nefkens, *Phys. Rev. C* **51**, 2310 (1995); **57**, 1004(E) (1998).
- [15] T. Feuster and U. Mosel, *Phys. Rev. C* **58**, 457 (1998).
- [16] T. Sato and T.-S. H. Lee, *J. Phys. G* **36**, 073001 (2009).
- [17] H. Kamano, S. X. Nakamura, T.-S. H. Lee, and T. Sato, *Phys. Rev. C* **88**, 035209 (2013).
- [18] D. Rönchen, M. Döring, F. Huang, H. Haberzettl, J. Haidenbauer, C. Hanhart, S. Krewald, U. -G. Meißner, and K. Nakayama, *Eur. Phys. J. A* **49**, 44 (2013).
- [19] S. N. Yang, S. S. Kamalov, and L. Tiator, *AIP Conf. Proc.* **1432**, 293 (2012).
- [20] T. P. Vrana, S. A. Dytman, and T. S. H. Lee, *Phys. Rep.* **328**, 181 (2000).
- [21] W.-T. Chiang, B. Saghai, F. Tabakin, and T. S. H. Lee, *Phys. Rev. C* **69**, 065208 (2004).
- [22] K. P. Khemchandani, A. Martinez Torres, and E. Oset, *Eur. Phys. J. A* **37**, 233 (2008).
- [23] K. Tsushima, A. Sibirtsev, A. W. Thomas, and G. Q. Li, *Phys. Rev. C* **59**, 369 (1999); **61**, 029903(E) (2000); K. Tsushima, S. W. Huang, and A. Faessler, *Phys. Lett. B* **337**, 245 (1994); *J. Phys. G* **21**, 33 (1995); *Aust. J. Phys.* **50**, 35 (1997); R. Shyam, *Phys. Rev. C* **60**, 055213 (1999).
- [24] R. Shyam, H. Lenske, and U. Mosel, *Phys. Rev. C* **77**, 052201 (2008); R. Shyam, K. Tsushima, and A. W. Thomas, *Phys. Lett. B* **676**, 51 (2009); R. Shyam, O. Scholten, and H. Lenske, *Phys. Rev. C* **81**, 015204 (2010).
- [25] R. A. Arndt, W. J. Briscoe, I. I. Strakovsky, and R. L. Workman, *Phys. Rev. C* **74**, 045205 (2006).
- [26] D. Diakonov, V. Petrov, and M. V. Polyakov, *Z. Phys. A* **359**, 305 (1997); M. V. Polyakov, A. Sibirtsev, K. Tsushima, W. Cassing, and K. Goetze, *Eur. Phys. J. A* **9**, 115 (2000); K. Goetze, H.-C. Kim, M. Praszalowicz, and G.-S. Yang, *Prog. Part. Nucl. Phys.* **55**, 350 (2005).
- [27] K. H. Hicks, *Eur. Phys. J. H* **37**, 1 (2012).
- [28] R. G. Edwards, J. J. Dudek, D. G. Richards, and S. J. Wallace, *Phys. Rev. D* **84**, 074508 (2011).
- [29] S. Capstick and W. Roberts, *Prog. Part. Nucl. Phys.* **45**, S241 (2000).
- [30] R. Koniuk and N. Isgur, *Phys. Rev. D* **21**, 1868 (1980); **23**, 818(E) (1981); N. Isgur and G. Karl, *Phys. Rev. D* **19**, 2653 (1979); **23**817(E) (1981).
- [31] N. Suzuki, B. Julia-Diaz, H. Kamano, T.-S. H. Lee, A. Matsuyama, and T. Sato, *Phys. Rev. Lett.* **104**, 042302 (2010); H. Kamano, S. X. Nakamura, T.-S. H. Lee, and T. Sato, *Phys. Rev. C* **81**, 065207 (2010).
- [32] N. Suzuki, T. Sato, and T.-S. H. Lee, *Phys. Rev. C* **82**, 045206 (2010).
- [33] D. J. Wilson, I. C. Cloet, L. Chang, and C. D. Roberts, *Phys. Rev. C* **85**, 025205 (2012).
- [34] I. G. Aznauryan *et al.* (CLAS Collaboration), *Phys. Rev. C* **80**, 055203 (2009).
- [35] D. Drechsel, S. S. Kamalov, and L. Tiator, *Eur. Phys. J. A* **34**, 69 (2007); L. Tiator, D. Drechsel, S. S. Kamalov, and M. Vanderhaeghen, *Chin. Phys. C* **33**, 1069 (2009).
- [36] S. Capstick and W. Roberts, *Phys. Rev. D* **47**, 1994 (1993).
- [37] S. Capstick and B. D. Keister, *Phys. Rev. D* **51**, 3598 (1995).
- [38] S. Capstick, T. S. H. Lee, W. Roberts, and A. Svarc, *Phys. Rev. C* **59**, R3002 (1999).
- [39] T. Melde, W. Plessas, and B. Sengl, *Phys. Rev. D* **77**, 114002 (2008).
- [40] E. Santopinto and M. M. Giannini, *Phys. Rev. C* **86**, 065202 (2012).
- [41] M. Ronniger and B. C. Metsch, *Eur. Phys. J. A* **49**, 8 (2013).
- [42] B. Golli and S. Sirca, *Eur. Phys. J. A* **38**, 271 (2008).
- [43] P. Alberto, M. Fiolhais, B. Golli, and J. Marques, *Phys. Lett. B* **523**, 273 (2001).
- [44] Y.-J. Zhang and B. Zhang, *Chin. Phys. C* **36**, 189 (2012).
- [45] R. Bijker, F. Iachello, and A. Leviatan, *Ann. Phys. (N.Y.)* **236**, 69 (1994); R. Bijker, F. Iachello, and A. Leviatan, *Ann. Phys. (N.Y.)* **284**, 89 (2000); E. Tomasi-Gustafsson, M. P. Rekalo, R. Bijker, A. Leviatan, and F. Iachello, *Phys. Rev. C* **59**, 1526 (1999).
- [46] R. Bijker, F. Iachello, and A. Leviatan, *Phys. Rev. C* **54**, 1935 (1996).
- [47] N. Matagne and F. Stancu, *Phys. Lett. B* **631**, 7 (2005).
- [48] D. S. Roberts, W. Kamleh, and D. B. Leinweber, [arXiv:1311.6626](https://arxiv.org/abs/1311.6626) [*Phys. Rev. D* (to be published)].
- [49] C. E. Carlson, *Phys. Rev. D* **34**, 2704 (1986); C. E. Carlson and J. L. Poor, *Phys. Rev. D* **38**, 2758 (1988); C. E. Carlson, *Few-Body Syst.* **11**, 10 (1999).
- [50] F. Gross, G. Ramalho, and M. T. Peña, *Phys. Rev. C* **77**, 015202 (2008).
- [51] G. Ramalho and K. Tsushima, *Phys. Rev. D* **81**, 074020 (2010).
- [52] F. Gross, *Phys. Rev.* **186**, 1448 (1969); A. Stadler, F. Gross, and M. Frank, *Phys. Rev. C* **56**, 2396 (1997).
- [53] F. Gross, G. Ramalho, and M. T. Peña, *Phys. Rev. D* **85**, 093005 (2012).
- [54] G. Ramalho, K. Tsushima, and F. Gross, *Phys. Rev. D* **80**, 033004 (2009).

- [55] G. Ramalho, M. T. Peña, and F. Gross, *Eur. Phys. J. A* **36**, 329 (2008).
- [56] G. Ramalho and M. T. Peña, *Phys. Rev. D* **80**, 013008 (2009).
- [57] G. Ramalho and M. T. Peña, [arXiv:1309.0730](https://arxiv.org/abs/1309.0730).
- [58] G. Ramalho and M. T. Peña, *Phys. Rev. D* **84**, 033007 (2011); G. Ramalho and K. Tsushima, *Phys. Rev. D* **84**, 051301 (2011); G. Ramalho, D. Jido, and K. Tsushima, *Phys. Rev. D* **85**, 093014 (2012).
- [59] G. Ramalho, M. T. Peña, and F. Gross, *Phys. Rev. D* **78**, 114017 (2008); G. Ramalho, M. T. Peña, and F. Gross, *Phys. Rev. D* **81**, 113011 (2010); G. Ramalho and M. T. Peña, *Phys. Rev. D* **85**, 113014 (2012); G. Ramalho, M. T. Peña, and A. Stadler, *Phys. Rev. D* **86**, 093022 (2012).
- [60] G. Ramalho and M. T. Peña, *J. Phys. G* **36**, 115011 (2009).
- [61] G. Ramalho and K. Tsushima, *Phys. Rev. D* **82**, 073007 (2010).
- [62] G. Ramalho and K. Tsushima, *Phys. Rev. D* **84**, 054014 (2011); G. Ramalho and K. Tsushima, *Phys. Rev. D* **86**, 114030 (2012); G. Ramalho, K. Tsushima, and A. W. Thomas, *J. Phys. G* **40**, 015102 (2013).
- [63] G. Ramalho and K. Tsushima, *Phys. Rev. D* **88**, 053002 (2013); G. Ramalho and K. Tsushima, *Phys. Rev. D* **87**, 093011 (2013).
- [64] G. Ramalho and M. T. Peña, *Phys. Rev. D* **83**, 054011 (2011).
- [65] J. J. Kelly, *Phys. Rev. C* **56**, 2672 (1997).
- [66] Z. Batiz and F. Gross, *Phys. Rev. C* **58**, 2963 (1998).
- [67] G. Ramalho and K. Tsushima, *AIP Conf. Proc.* **1374**, 353 (2011).
- [68] F. Gross, G. Ramalho, and M. T. Peña, *Phys. Rev. C* **77**, 035203 (2008).